# Effects of Silicon Content on Oxidation at 1000°C of Aisi 1045, Aisi 5160 and Aisi 9254 Steels.

Guilherme Maranhão Costa *, Lioudmila Aleksandrovna Matlakhova, Sergio Neves Monteiro

Posted Date: 8 December 2023

doi: 10.20944/preprints202312.0575.v1

Keywords: high-temperature; silicon; oxidation

*Article*

# Effects of Silicon Content on Oxidation at 1000 °C of AISI 1045, AISI 5160 and AISI 9254 Steels

**Guilherme Costa [1,*], Lioudmila Matlakhova [2] and Sergio Monteiro [3,*]**

[1] State University of North Fluminense Darcy Ribeiro-Brazil; guilherme.maranhao.costa@gmail.com
[2] State University of North Fluminense Darcy Ribeiro-Brazil; lioudmila@uenf.br
[3] Military Engineering Institute-Brazil; sergio.neves@ime.eb.br
* Correspondence: guilherme.maranhao.costa@gmail.com

**Abstract:** The main objective was to analyze the influence of silicon content on high-temperature oxidation of low-alloy steels. Samples of AISI 1045, AISI 5160, and AISI 9254 steels, with different silicon contents, were oxidized at an isothermal temperature of 1000°C for times of 20 minutes, 40 minutes, and 60 minutes. The oxide layers formed mainly contain hematite, magnetite wustite, and fayalite. The average thickness of the oxide layer can decrease with an increase in silicon content below 1% but can increase for contents greater than 1% due to the difference in density between fayalite and iron oxides. Silicon tends to accumulate on the surface of steel and form a $SiO_2$ film in the early stages of oxidation, which can control the oxidation process. The eutectic compound $FeO+Fe_2SiO_4$ forms at the oxide-steel interface, and its thickness increases with oxidation time and the silicon content present. The $SiO_2$ film tends to decrease with oxidation time and silicon content.

**Keywords:** high-temperature; silicon; oxidation

## 1. Introduction

Silicon is an element commonly present in low-carbon steels and is generally added to increase resistance to high temperatures, and oxidation, and improve the mechanical properties of the alloy [1,2]. However, in processes that occur at high temperatures, such as hot rolling, a layer of oxides called red scale is formed, which has high mechanical properties. This layer appears due to the formation of the compound fayalite ($Fe_2SiO_4$), coming from the combination of silicon dioxide ($SiO_2$) and wustite (FeO), presenting high adhesion to the metal substrate [3,4]. The presence of the red scale layer increases the oxidation resistance of the alloy, as it slows down the diffusion of Fe ions to the surface of the metallic substrate and hinders the interaction of oxygen with the metallic compounds present. On the other hand, it is difficult to remove, which implies longer cleaning time and higher processing costs [5,6]. This is due formation of the eutectic $FeO+Fe_2SiO_4$ which is high to the substrate and makes it difficult to completely remove the oxide layer during processing [7]. Some studies have focused on evaluating the influence of silicon on the oxidation process.

Suarez et. al. [8], evaluated additions of different amounts of silicon to iron subjected to temperatures between 900-1200°C. The results showed that in low quantities the oxide layer formed presents the three classic iron oxides (Wustite, magnetite, and hematite), with the presence of silicates in the contours of the oxide crystals. Higher percentages of silicon resulted in the reaction between wustite and silicate compounds, with the formation of fayalite. The amount of fayalite present increases proportionally to the increase in silicon content, which leads to a reduction in the oxidation rate, reducing the thickness of the oxide layer.

Fukagawa et. al. [9], analyzed the formation of red scale during hot rolling of steel. The authors pointed out that the formation of the red scale occurs due to the difficulty in completely removing the FeO layer formed during reheating for rolling. This is due to the formation of the eutectic compound $FeO+Fe_2SiO_4$, as fayalite forms between the metallic substrate and the oxide layer, presenting high adhesion, and penetrates irregularly through the FeO layer, making it difficult to remove from the surface.

 doi:10.20944/preprints202312.0575.v1



Liu et. al. [10] studied the oxidation at high temperatures of a Fe-1.5%Si alloy. The authors observed that between 700-900°C, two layers of oxides are formed, an outer layer composed of iron oxides, and an inner layer composed of $FeO+Fe_2SiO_4$ with silicon oxide precipitates. From 1000° onwards, silicon precipitates dissolve in the internal $FeO+Fe_2SiO_4$ layer. Above 1200°C the $FeO+Fe_2SiO_4$ compound penetrates deeply into the external layer of Fe oxides. The temperature range of 700-1100° proved to be the most suitable, with the formation and growth of the $FeO+Fe_2SiO_4$ layer making the process of oxidation. However, above 1200°C the Pilling-Bedworth ratio of the oxide layer is greater than 1, resulting in compressive stresses that increase the oxidation rate, and the oxide layer loses its ability to protect against corrosion.

The studies carried out to date have used oxidizing atmospheres only from the moment the isothermal temperature was reached, whereas in an industrial environment, the oxidizing atmosphere is present throughout the entire heating process. Furthermore, most of the heating cycles used do not resemble those applied by industry, where steels are subjected to temperatures ranging from atmospheric temperatures to high temperatures. The objective of this study is to evaluate the influence of silicon on the oxidation process of low-carbon steels, using atmospheres and temperatures similar to those used in industry for the heating process. To achieve this, samples of three low-carbon steels with similar compositions, but different percentages of silicon, were subjected to oxidation at high temperatures, using reheating cycles, temperatures, and atmospheres similar to those used in industrial environments.

## 2. Materials and Methods

The oxidation tests were carried out on AISI 1045, AISI 5160, and AISI 9254 steel samples, with different percentages of silicon. The materials were obtained from a commercial supplier, and their compositions are detailed in Table 1. The steel samples used were cylindrical, 15 mm in diameter, and 15 mm in length. Before the oxidation tests, the samples were sanded and subsequently polished to remove surface inconsistencies and discontinuities that could interfere with the formation and analysis of the oxide layer.

**Table 1.** Chemical composition of the steels (wt.%).

| Steel | C | Mn | Si | P | S | Ni | Mo |
|---|---|---|---|---|---|---|---|
| AISI 1045 | 0,43 | 0,71 | 0,02 | 0,018 | 0,025 | 0,08 | 0,020 |
| AISI 51160 | 0,57 | 0,78 | 0,22 | 0,021 | 0,024 | 0,07 | 0,013 |
| AISI 9254 | 0,55 | 0,67 | 1,34 | 0,014 | 0,008 | 0,01 | 0,006 |

The samples were then subjected to oxidation in an oven, in the presence of atmospheric air, at a heating rate of 20°C/min until reaching an isothermal temperature of 1000°C, being maintained at this temperature level for periods of 20 minutes, 40 minutes, and 60 minutes, and then cooled at a cooling rate of 20°C/min to avoid thermal shock. Figure 1 shows the oxidation routines used.

Preprints (www.preprints.org) | NOT PEER-REVIEWED | Posted: 8 December 2023 doi:10.20944/preprints202312.0575.v1



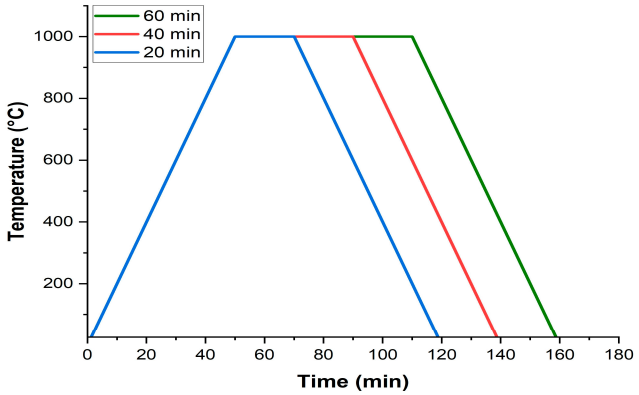


**Figure 1.** Oxidation routines.

After the oxidation tests, the samples were analyzed to evaluate the oxide layers formed. The oxide layer's surface of the samples was analyzed by X-ray diffraction (XRD) to determine the phases present. The samples were then embedded in conductive resin, to protect the oxide layer and enable the evaluation of the cross sections. Subsequently, the samples were sanded and polished, and the microstructure and morphology of the oxide layer were analyzed by scanning electron microscopy (SEM) and optical microscopy. From the cross-section images it was possible to determine the thickness of the oxide layer and the eutectic FeO+ $Fe_2SiO_4$ layer. The distribution of chemical elements was analyzed by energy dispersive spectroscopy (EDS) to determine the penetration depth of the $Fe_2SiO_4$ layer.

## 3. Results and Discussion

### *3.1. XDR analysis*

Figure 2 displays the diffractogram obtained by XRD from the surface of the oxide layer of the AISI 1045 steel sample.

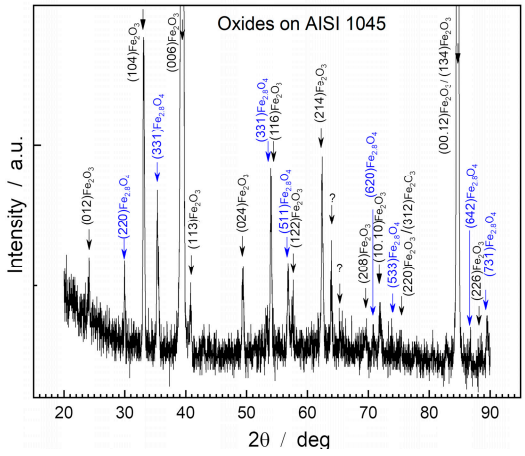


**Figure 2.** Diffractogram of the oxide layer formed on AISI 1045 steel after 60 minutes of exposure to an isothermal temperature of 1000°C.

The oxide layer of AISI 1045 steel presented two main phases: hematite ($Fe_2O_3$) and magnetite ($Fe_3O_4$), with a predominance of the compounds $Fe_2O_3$ (PDF 87-1166), $Fe_{2,886}$ $O_4$ (PDF 86-1342) and $Fe_3O_4$ (PDF 88 -0315).

Hematite is the predominant compound in the oxide layer due to the high intensity of the corresponding peaks, in which the crystallographic planes (006) $Fe_2O_3$ stand out, with an intensity (I) of 17,620.4 a.u; (00.12) $Fe_2O_3$, with I=1,285.0 a.u; and (134) $Fe_2O_3$, with I=654 a.u. The intensity of these

Preprints (www.preprints.org) | NOT PEER-REVIEWED | Posted: 8 December 2023 doi:10.20944/preprints202312.0575.v1



peaks indicates that hematite has preferential crystallographic planes in relation to the steel surface or other intermediate compounds, such as $Fe_{2.886}O_4/Fe_3O_4$.

Figure 3 shows the diffractogram obtained through XRD of the surface of the oxide layer of the AISI 5160 steel sample.

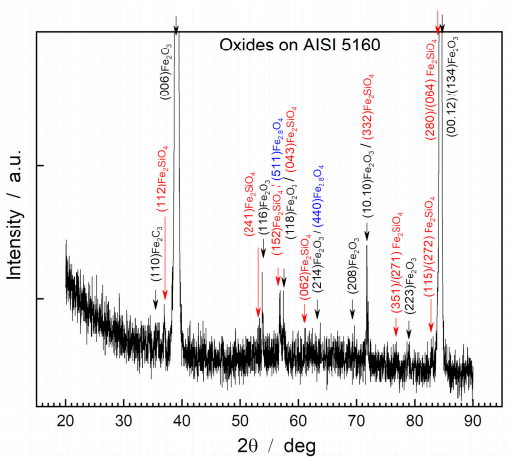


**Figure 3.** Diffractogram of the oxide layer formed on AISI 5160 steel after 60 minutes of exposure to an isothermal temperature of 1000°C.

XRD analysis of the oxide layer's surface of AISI 5160 steel showed the presence of hematite, magnetite, and fayalite under the form of the compounds $Fe_2O_3$ (PDF 87-1166), $Fe_{2.886}O_4$ (PDF 86-1342), and $Fe_2SiO_4$ (PDF 01-070-1861).

On the surface of the oxide layer, hematite predominates as the main compound due to the significantly higher intensity of its peaks compared to other compounds present. This phenomenon also occurs in the case of AISI 1045 steel, where the intensities of the hematite peaks serve as indicators of the preferential orientation of the crystalline lattice in relation to the steel surface.

The highest intensity peaks are those belonging to the characteristic planes (006) $Fe_2O_3$, with I=17,620.4 a.u; (00.12) $Fe_2O_3$, with I=1,285.0 a.u; and (134) $Fe_2O_3$, with I=654 a.u.

Figure 4 shows the diffractogram obtained through XRD of the surface of the oxide layer of the AISI 9254 steel sample.

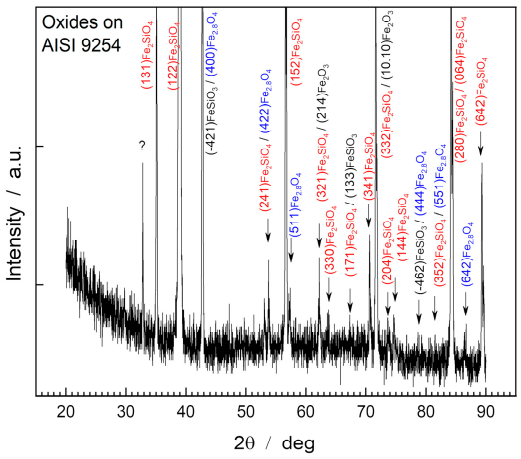


**Figure 4.** Diffractogram of the oxide layer formed on AISI 9254 steel after 60 minutes of exposure to an isothermal temperature of 1000°C.

In the AISI 9254 steel sample, the diffraction patterns showed peaks relating to magnetite, hematite, fayalite, and iron metasilicate. The compounds identified were $Fe_2O_3$ (PDF 87-1166), $Fe_{2,886}O_4$ (PDF 86-1342), $Fe_2SiO_4$ (PDF 01-070-1861) and $FeSiO_3$ (PDF 82-1834). The oxide layer presents

 doi:10.20944/preprints202312.0575.v1



a greater share of fayalite ($Fe_2SiO_4$), which is evidenced by the presence of high-intensity peaks of this compound.

The increase in silicon content causes changes in the phase composition of the steel oxide layers, as demonstrated when comparing the analysis results. When comparing AISI 1045 and AISI 5160 steels, a 0.1% increase in silicon content resulted in a decrease in the amounts of hematite and magnetite generated during oxidation. This allowed the first peaks of the fayalite phase to emerge, although with lower intensity than other oxides present. In the case of AISI 9254 steel, with an increase in silicon content (1.34% Si), fayalite became the predominant phase in the oxides, exhibiting more intense peaks. This pattern suggests that increasing silicon reduces the formation of magnetite, hematite, and possibly other compounds during oxidation. This is reinforced by the fact that fayalite formation occurs close to the interface between the steel and the oxide layer. In situations of thin layers or low silicon content, fayalite may not be detected due to limited X-ray penetration. Therefore, the decrease in hematite and magnetite, together with an increase in fayalite, facilitated the identification of peaks associated with the $Fe_2SiO_4$ compound.

### *3.2. Cross-Section Microstructural Characterization*

Figure 5 shows the cross-section of steel samples oxidized at an isothermal temperature of 1000°C for different exposure times.

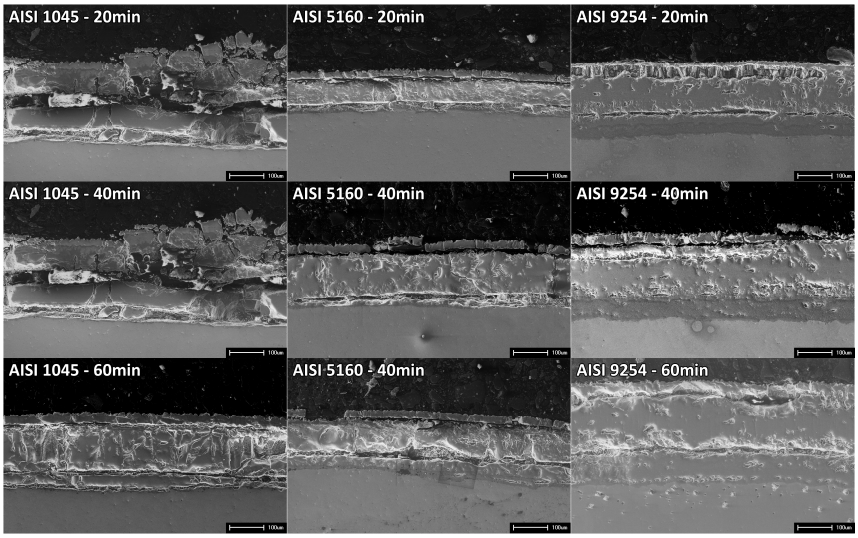


**Figure 5.** Oxide layers' cross-section of AISI 1045, AISI 5160, and AISI 9254 steels were subjected to an isothermal temperature of 1000°C for 20 minutes, 40 minutes, and 60 minutes.

The oxide layers formed have a distribution with an outer layer composed of Hematite ($Fe_2O_3$), an intermediate layer formed by Magnetite ($Fe_3O_4$), and an internal layer formed by a thin film of $SiO_2$, Fayalite ($Fe_2SiO_4$), and the eutectic $FeO+Fe_2SiO_4$. The Magnetite layer is predominant in the oxide layer, being considerably thicker than the other layers. Hematite is found on the surface of the oxide layer, being relatively thin, fragile, and with low adhesion.

The Hematite layer present on the surface of the oxide layer reveals different characteristics in relation to the other layers. When compared to the underlying Magnetite layer, the thickness of the Hematite layer is considerably smaller. Furthermore, its fragility is notable, with some regions appearing to be partially detached from the rest of the oxide layer. These indications suggest that the outer layer has a significantly reduced adhesion in relation to the adjacent layers. Furthermore, most of the apparent discontinuities are concentrated in the outermost layers, composed mainly of hematite and magnetite. These layers are more vulnerable and exhibit relatively low adhesion compared to the inner layers of the oxide layer. It is important to highlight, however, that only a

 doi:10.20944/preprints202312.0575.v1



limited amount of oxides suffered detachment, indicating that, despite low adhesion, the overall integrity of the oxide layer was preserved for the most part.

The increase in the exposure time to isothermal temperature results in greater thicknesses of the oxide layer since the iron and oxygen ions have more time to diffuse and continue the oxidation process [11]. Exposure time also had effects on the integrity of the oxide layer of SAE 1045 steel. For shorter exposure times, the oxide layer presented a greater number of regions with high amounts of cracks and oxide detachment, making it difficult to carry out accurate thickness measurements of the layer. However, for a time of 60 minutes, the oxide layer showed greater integrity, although it continued to have a low level of adhesion to the metal substrate.

The increase in Si content resulted in greater integrity and adhesion of the oxide layers formed on the AISI 5160 and AISI 9254 steels, with fewer discontinuities detected and a smaller amount of oxide detachment. These characteristics indicate an increase in the oxidation resistance of the alloy.

Figure 6 shows the regions of the oxide-steel interface of the AISI 1045, AISI 5160, and AISI 9254 steel samples exposed to an isothermal temperature of 1000°EC for times of 20 minutes, 40 minutes, and 60 minutes.

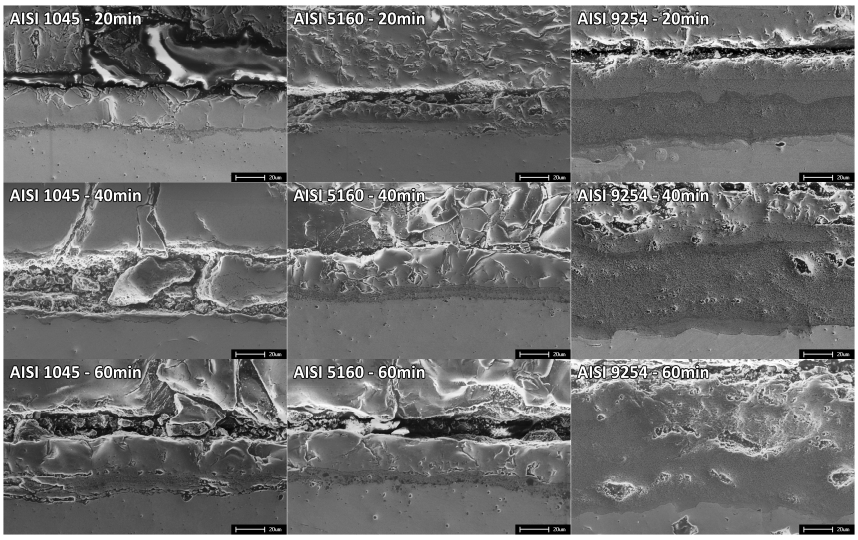


**Figure 6.** Oxide-steel interface of AISI 1045, AISI 5160, and AISI 9254 steels subjected to an isothermal temperature of 1000°C.

An analysis of the oxide-steel interface of AISI 1045 steel shows that, despite the low percentage of Si (0.1% Si), the formation of the eutectic $FeO+Fe_2SiO_4$ linked to the metallic substrate is still possible. notice a darker region between the eutectic and the other layers, which can be attributed to $SiO_2$. The greater diffusivity of Si in relation to Fe allows it to accumulate in the surface region of the steel, which during the oxidation process reacts with $O_2$ to form $SiO_2$, and with the process community the formation of fayalite.

The inner layer is notable for its high level of adhesion to the metal substrate. According to the $FeO+Fe_2SiO_4$ phase diagram, we can anticipate the presence of two distinct phases in this layer: wustite (FeO) and fayalite ($Fe_2SiO_4$). Furthermore, the formation of the eutectic $FeO+Fe_2SiO_4$ at the interface between these phases is expected, indicating a complex interaction between the constituents of the inner layer and their adhesion properties to the metallic substrate.

The silicon content had a significant effect on the thickness of the phases that make up the oxide layer. Figure 7 shows the cross-section of the samples oxidized with exposure time at an isothermal temperature of 1000°C for 40 min.

Preprints (www.preprints.org) | NOT PEER-REVIEWED | Posted: 8 December 2023 doi:10.20944/preprints202312.0575.v1



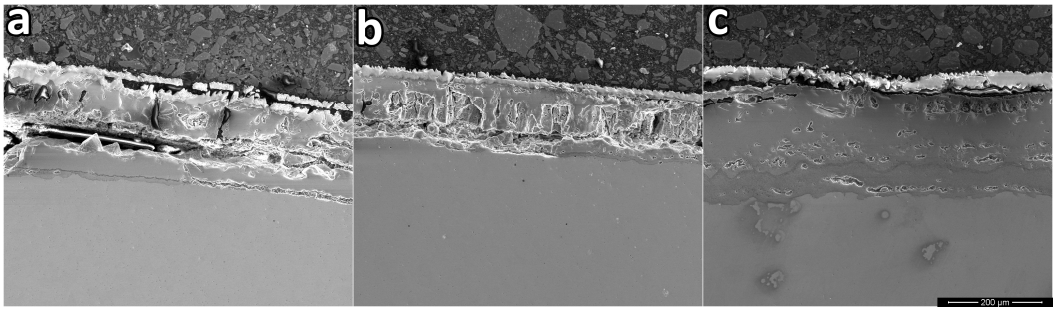


**Figure 7.** Cross section of the oxide layer after exposure time to isothermal temperature of 40 minutes.

Through Figure 7 it is possible to see two main effects of increasing the silicon content, the reduction of defects such as cracks, voids, and pores, and a variation in the thickness of the oxide layer. A smaller number of defects leads to an increase in the mechanical resistance of the oxide layer, which can better accommodate the thermal or mechanical stresses generated during the oxidation process, which could result in large cracks or detachment of the oxide layer, which could accelerate the oxidation process.

Regarding the effect of silicon on the thickness of the oxide layer, Figure 8 shows the graph of the variation in the average thickness as a function of time and silicon content.

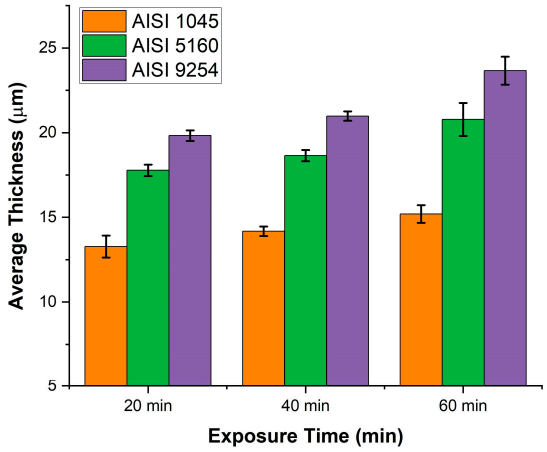


**Figure 8.** Average thickness of the oxide layer as a function of time and silicon content.

As can be seen in Figure 8, regardless of the exposure time, when the silicon content increases from 0.1% to 0.22% there is a decrease in the thickness of the oxide layer, however, when the silicon content increases from 0.22% % to 1.34% the opposite occurs, an increase in the thickness of the oxide layer. The increase in the thickness of the oxide layer when the silicon content increases from 0.22% to 1.34% is related to the amount of Fayalite formed during oxidation.

Compared to the outer layers, the inner layer showed significant variations, depending on time and silicon content. In the case of SAE 1045 steel, with a lower silicon content, oxidation led to the formation of thin layers of $SiO_2$ and the $FeO+Fe_2SiO_4$ system, but with a significantly smaller thickness compared to other oxides, which does not offer protection. strong against oxidation.

The oxide layers formed on SAE 5160 steel showed the formation of the eutectic $FeO+Fe_2SiO_4$ in all time ranges. The inner layer is formed by the eutectic $FeO+Fe_2SiO_4$ at the interface with the steel and the $SiO_2$ film. The thickness of the $FeO+Fe2SiO_4$ eutectic was relatively greater compared to the thickness of the oxide layer of the SAE 1045 steel, even with the small difference in the Si content.

Among the oxide layers formed, those of SAE 9254 steel were the ones that showed the formation of the largest amount of Fayalite, and consequently of the eutectic $FeO+Fe_2SiO_4$, due to the higher

Preprints (www.preprints.org) | NOT PEER-REVIEWED | Posted: 8 December 2023 doi:10.20944/preprints202312.0575.v1



silicon content present. The thickness of the eutectic constituent is comparable to that of other oxides, contributing to greater resistance to oxidation of the alloy.

Figure 9 shows a comparative graph of the thickness of the eutectic constituent $FeO+Fe_2SiO_4$ as a function of time and silicon content.

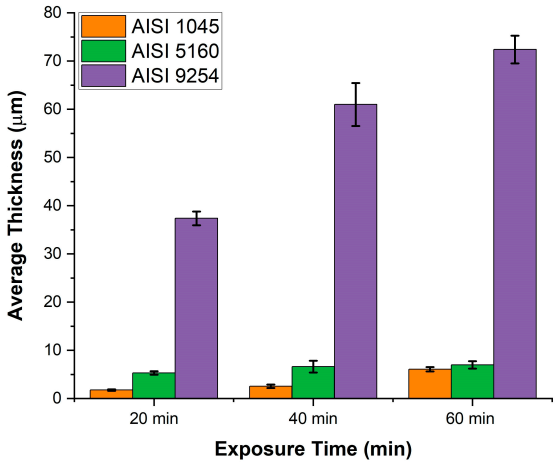


**Figure 9.** The average thickness of the eutectic $FeO+Fe_2SiO_4$ as a function of time and silicon content.

Time and silicon content have a significant impact on the thickness of the $FeO+Fe_2SiO_4$ eutectic. In this case, silicon plays the main role, with the increase in its content resulting in increases in the eutectic thickness of around 1000% in some measurements. The thickness of the $FeO+Fe_2SiO_4$ eutectic layer is directly related to the silicon content. With higher levels, more silicon is available to diffuse, giving rise to a greater amount of $SiO_2$, which during continued oxidation will react with iron and Wustite, giving rise to a greater amount of Fayalite, resulting in a eutectic $FeO+Fe_2SiO_4$ thicker.

Another important aspect to be highlighted is the shape of the $FeO+Fe_2SiO_4$ eutectic grains, which, regardless of time and silicon content, appear as fine Wustite grains in a Fayalite matrix. This format can be explained by the diffusion of Si ions. When temperatures between 950-1050°C are reached, depending on the composition of the alloy, silica reacts with iron ions resulting in iron and silicon oxide, which accumulates at the interface. As the oxidation process continues, silicon begins to diffuse along the grain boundaries of the Wustite layer. The silicon then reacts with Wustite, forming Fayalite, which starts to grow in the grain boundaries of Wustite, giving rise to the aesthetic system $FeO+Fe_2SiO_4$, with the shape of fine grains of Wustite dispersed in the Fayalite matrix.

The oxide layers showed the formation of Hematite and Magnetite, regardless of time and Si content, which showed greater fragility, several defects (pores, cracks, and voids), and less adhesion to other layers, which can result in detachment, decreasing oxidation resistance.

The formation of the internal layer occurs at the oxide-steel interface, and its growth is dependent on the diffusion of Fe ions. As these ions diffuse preferentially through defects such as grain boundaries, cracks, and pores, the continuity of the oxidation process becomes highly dependent on the density of defects that the oxide layer presents [13].

The high adhesion presented by the internal layer is the result of two main factors, the low level of porosity presented and the anchoring effect of Fayalite. Pores act as a preferential path for oxygen diffusion [3] and also affect the mechanical properties of the oxide layer as they act as stress concentrators, reducing mechanical resistance, and leaving the oxide layer more susceptible to cracking and oxide detachment [14]. The anchoring effect is related to the formation of Fayalite at the Wustite grain boundaries, trapping these grains. The eutectic $FeO+Fe_2SiO_4$ generated has high mechanical resistance, withstanding higher levels of stress. On the other hand, the presence of the eutectic $FeO+Fe_2SiO_4$ makes it difficult to remove the oxide layer due to the anchoring effect [9].

The reduction in the number of defects can be explained by the formation of $SiO_2$, which increases the oxidation resistance of the alloy by filling cracks, pores, and voids, resulting in a

 doi:10.20944/preprints202312.0575.v1



reduction in the density of defects in the oxide layer, and consequently reducing the diffusivity of oxygen and iron ions [15].

Changes in the thickness of the oxide layer may be related to the density of the oxides generated. Fayalite has a density of about 3.85g/cm³, while the density of iron oxides is about 5.24g/cm³ for hematite, 5.17g/cm³ for magnetite, and 5.75g/cm³ for wustite. As the increase in Si content results in the formation of greater amounts of $SiO_2$, and consequently greater amounts of fayalite. The volume of oxide generated from the formation of fayalite is greater than the volume of oxide consumed, which increases the thickness of the $FeO+Fe_2SiO_4$ eutectic layer, as occurs with the oxide layer of SAE 9254 steel, which has the highest Si content.

### *3.3. Chemical Characterization*

Figure 10 shows the cross-section of the AISI 1045 steel samples oxidized at different times of exposure to isothermal temperature.

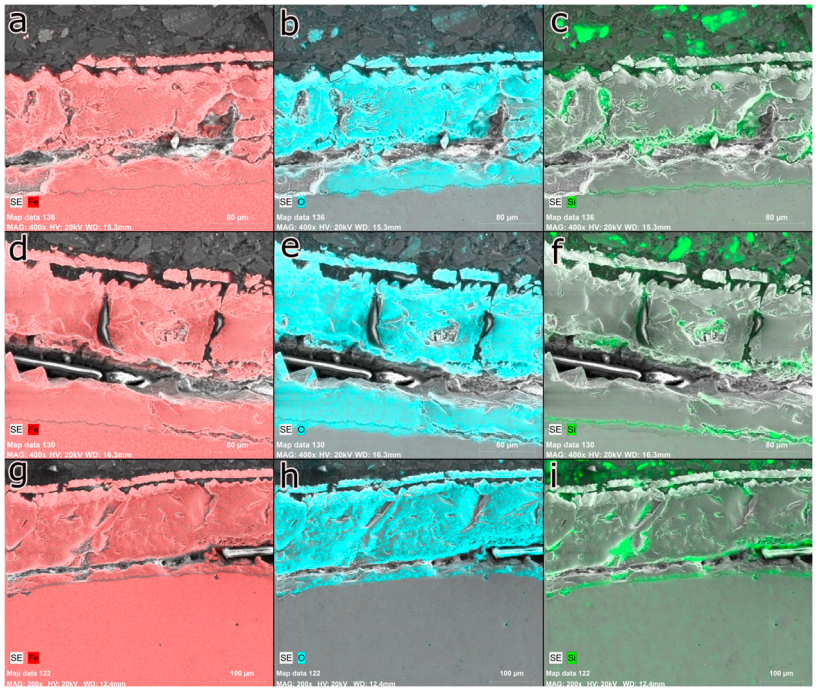


**Figure 10.** EDS analysis of AISI 1045 steel cross-section: a) Fe-20min, b) O-20 min, c) Si-20min, d) Fe-40min, e) O-40 min, f) Si-40min, g) Fe-60min, h) O-60min, i) Si-60min.

When carrying out a detailed analysis of the cross-section of the oxide layer, the presence and distribution of three primary chemical elements become evident: iron, oxygen, and silicon. Both iron and oxygen are uniformly dispersed throughout the oxide layer. However, it is important to highlight that there is a delicate layer, located close to the oxide interface, which is characterized by a low concentration of iron and a high concentration of silicon. This particularity configures a specific chemical configuration in this region of the oxide layer.

In general, the distribution of iron, oxygen, and silicon showed few significant variations with increasing time. The inner oxide layer is predominantly composed of $SiO_2$ and the eutectic compound. It is worth mentioning that the thickness of the eutectic compound layer tends to increase with increasing temperature. Even though it has a low silicon content, it is common to observe that this element diffuses and segregates on the steel surface, reacting with oxygen and forming a $SiO_2$ film. It is important to highlight that this characteristic is independent of time. Throughout the oxidation process, both iron and oxygen diffuse through the $SiO_2$ film, forming iron oxides and fayalite, which increases the total thickness of the oxide layer.

From the analysis of the interface region, it was verified the existence of a layer close to the substrate that has a low iron content and a high silicon content. This fact suggests that the layer is

 doi:10.20944/preprints202312.0575.v1



mostly made up of $SiO_2$ since there is the presence of oxygen in the region. Just below the $SiO_2$ layer, it is possible to observe the presence of some regions formed by the eutectic compound $FeO+Fe_2SiO_4$, which has the typical shape of rounded wustite grains, surrounded by a fayalite matrix. It is interesting to note that, despite the low silicon content, the presence of wustite between the $SiO_2$ film and the steel is relatively low, which suggests a low diffusivity of the elements that participate in the oxidation process.

Figure 11 shows the cross-section of the AISI 5160 steel samples oxidized at different exposure times. Silicon maintains its characteristic of concentrating at the steel-oxide interface, even for the shortest exposure time. It is also possible to observe the low presence of iron at the steel-oxide interface, indicating the presence of the $SiO_2$ film.

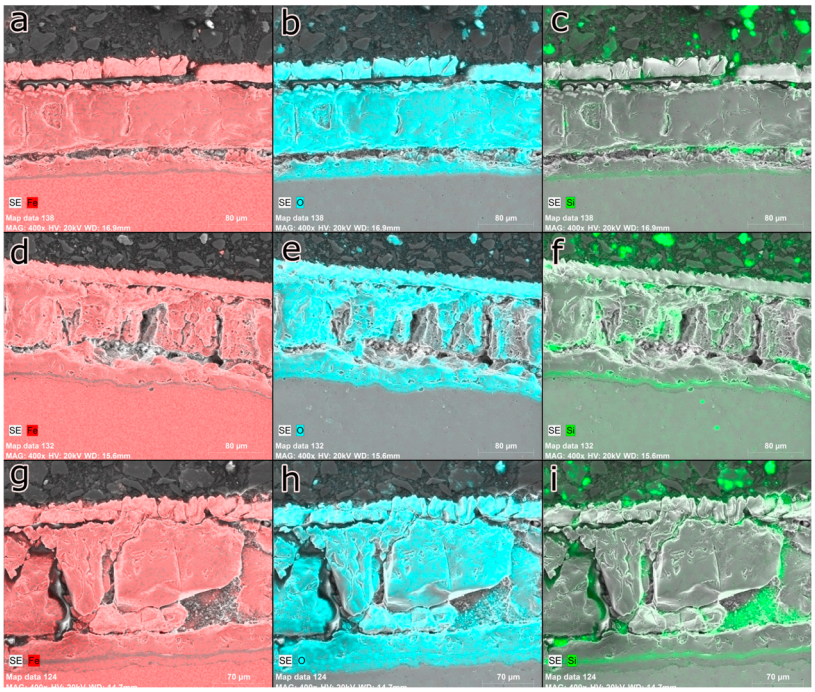


**Figure 11.** EDS analysis of AISI 5160 steel cross-section: a) Fe-20min, b) O-20 min, c) Si-20min, d) Fe-40min, e) O-40 min, f) Si-40min, g) Fe-60min, h) O-60min, i) Si-60min.

The inner layer is composed of a thin film of $SiO_2$, followed by the eutectic compound and, finally, a layer of wustite. Furthermore, it is possible to observe that silicon was concentrated in certain regions of the oxide-steel interface, a behavior that was also observed at all times. However, at 60 minutes, silicon showed a more intense concentration in these regions of the interface, which suggests that prolonged oxidation increased the tendency of silicon to concentrate in these regions. This behavior can be attributed to the diffusion of silicon from the metal matrix to the oxide layer, which occurs under high-temperature conditions. The concentration of silicon at the oxide-steel interface can affect the properties of the oxide layer and, consequently, the corrosion and oxidation resistance of the material.

Figure 12 shows the cross-section of the AISI 9254 steel samples oxidized by different times of exposure to isothermal temperature.

Preprints (www.preprints.org) | NOT PEER-REVIEWED | Posted: 8 December 2023 doi:10.20944/preprints202312.0575.v1



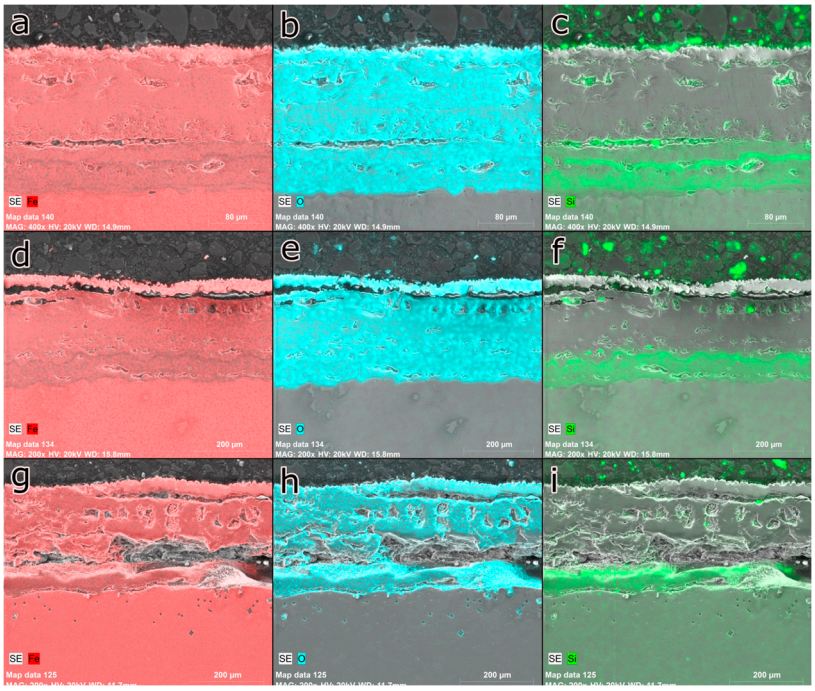


**Figure 12.** EDS analysis of AISI 9254 steel cross-section: a) Fe-20min, b) O-20 min, c) Si-20min, d) Fe-40min, e) O-40 min, f) Si-40min, g) Fe-60min, h) O-60min, i) Si-60min.

Silicon maintained the tendency to concentrate at the interface with the eutectic compound. This behavior indicates that this region is mostly composed of $SiO_2$, which is evident from the low concentration of iron in this region. As the silicon becomes concentrated on the surface, the formation of fayalite occurs more easily as the temperature rises and the oxidation process continues [16]. When reaching a temperature of 800°C, the silicon that has diffused through the wustite grain boundaries reacts to form fayalite, which gives rise to the eutectic compound.

The increase in time in the oxidation process of AISI 9254 steel has a significant effect on longer exposure times to isothermal temperatures. The increase in exposure time from 20 to 40 minutes did not result in changes, with the silicon concentrating at the interface with the eutectic compound. However, with an increase in the oxidation time to 60 minutes, the silicon began to be distributed uniformly throughout the region of the eutectic compound, as shown in Figure 60. In this case, the longer oxidation time allowed a greater amount of $SiO_2$ to react to form fayalite, thereby decreasing the Si concentration at the interface with the eutectic compound. This behavior allowed the thickness of the eutectic compound to increase considerably, which may contribute to an increase in oxidation resistance.

Most of the silicon is concentrated close to the oxide-steel interface, which is due to the formation of the $SiO_2$ layer in the initial stages of oxidation. Despite the amount of silicon present, the tendency is for the formation of a $SiO_2$ film, segregation and diffusion of silicon, and formation of fayalite with increasing temperature.

The chemical distribution profile follows the pattern composed of a $SiO_2$ film between the eutectic compound and the other oxide layers, evidenced by the region of low iron concentration, and by the eutectic compound $FeO+Fe_2SiO_4$ on the metallic substrate, evidenced by the presence of silicon distributed in the form of a matrix that surrounds the wustite grains.

Based on the analysis of AISI 1045 steel, it is evident that, despite the low Si content, the formation of a $SiO_2$ film occurs, however, the amount of fayalite formed was relatively low, with the thickness of the eutectic compound being similar to that of $SiO_2$ film. When we compare the three steels, it is possible to observe that the immediate effect of increasing the Si content is the increase in the thickness of the eutectic compound, in addition to this, there is a reduction in the $SiO_2$ film, whose efficiency in protecting against corrosion is also reduced.

 doi:10.20944/preprints202312.0575.v1



In general, the oxidation time affected the distribution of chemical elements only in the interface region. The region of the eutectic compound tends to grow with increasing oxidation time due to the reduction of the $SiO_2$ film that reacts with iron resulting in the segregation of silicon or the formation of fayalite. The formation of the $SiO_2$ film in the initial stages of oxidation is related to the diffusivity presented by silicon. Unlike elements such as manganese, cobalt, nickel, and molybdenum, which have diffusion coefficients close to the self-diffusion coefficient of iron, silicon presents considerably higher values for the same parameters. This behavior is due to the fact that the silicon atom has a significantly smaller size compared to other metals [17].

The presence of higher silicon contents resulted in a greater amount of fayalite and a reduction in the thickness of the $SiO_2$ layer. Depending on the silicon content, as well as the temperature and oxidation time, the $SiO_2$ film may disappear completely, as in the case of the AISI 9254 steel sample oxidized for 60 minutes.

The reduction of the $SiO_2$ film is the result of the formation of a greater amount of fayalite, which consequently leads to a greater thickness of the eutectic compound. The eutectic compound wustite-fayalite has been shown to have a significant influence on the oxidation process of low alloy steels at high temperatures. In general, the presence of this eutectic compound in the steel microstructure can delay the formation of oxide layers and, consequently, reduce the oxidation rate through the formation of complex mixed oxides that are more resistant to oxidation. Furthermore, the presence of the eutectic compound can change the morphology of the oxides formed, which can increase the adhesion of these oxides to the steel surface, further contributing to the reduction of the oxidation rate [18].

However, it is important to highlight that the influence of the eutectic compound wustite-fayalite on the oxidation process may vary depending on the conditions of exposure to high temperatures, and the chemical composition of the steel and microstructure [19].

## 6. Conclusions

From the analysis of the results obtained in the present study, it is possible to infer the following conclusions:

- The layer of oxides generated by the oxidation process showed the formation of the characteristic iron oxides, hematite, magnetite, and wustite. However, the amount of wustite generated was relatively lower compared to literature reports, which can be attributed to the formation of a $SiO_2$ layer in the initial stages of oxidation.
- The thickness of the hematite and magnetite layers tends to decrease with increasing silicon content, making it possible to identify the other phases present by XRD.
- The average thickness of the oxide layer tends to decrease when the silicon content increases to values below 1%. However, for levels above 1%, the thickness of the oxide layer may increase due to the difference in density between fayalite and iron oxides.
- The number of internal defects in the oxide layers was also reduced with increasing silicon content.
- At the interface between the oxide and the steel, the eutectic compound $FeO+Fe_2SiO_4$ is formed and the thickness tends to increase with longer exposure times to isothermal temperature of 1000°C and higher silicon contents.
- The presence of a $SiO_2$ film was detected in the oxide-steel interface region, where silicon tends to accumulate during the oxidation process. The $SiO_2$ film formed tends to decrease with increasing exposure time to the isothermal temperature of 1000°C and the silicon content, and in the case of the oxide layer formed on AISI 9254 steel, the $SiO_2$ film could not be identified.

## References

1. Nishimura, T. Rust Formation and Corrosion Performance of Si- and Al-Bearing Ultrafine Grained Weathering Steel. Corros. Sci. **2008**, 50 (5), 1306–1312. https://doi.org/10.1016/j.corsci.2008.01.025.

2. Yuan, Q.; Xu, G.; Liang, W.; Zhou, M.; Hu, H. Effects of Oxygen Concentration on the Passivation of Si-Containing Steel during High-Temperature Oxidation. Corros. Rev. **2018**, 36 (4), 385–393. https://doi.org/10.1515/corrrev-2017-0077.
3. Chen, R. Y.; Yuen, W. Y. D. Examination of Oxide Scales of Hot Rolled Steel Products. ISIJ Int. **2005**, 45 (1), 52–59. https://doi.org/10.2355/isijinternational.45.52.
4. Bolt, P. H. Understanding the Properties of Oxide Scales on Hot Rolled Steel Strip. steel Res. Int. **2004**, 75 (6), 399–404. https://doi.org/10.1002/srin.200405786.
5. Yang, Y.-L.; Yang, C.-H.; Lin, S.-N.; Chen, C.-H.; Tsai, W.-T. Effects of Si and Its Content on the Scale Formation on Hot-Rolled Steel Strips. Mater. Chem. Phys. **2008**, 112 (2), 566–571. https://doi.org/10.1016/j.matchemphys.2008.06.021.
6. Ros-Yañez, T.; Houbaert, Y.; Fischer, O.; Schneider, J. Production of High Silicon Steel for Electrical Applications by Thermomechanical Processing. J. Mater. Process. Technol. **2003**, 143–144 (1), 916–921. https://doi.org/10.1016/j.jmatprotec.2003.10.002.
7. Okada, H.; Fukagawa, T.; Ishihara, H.; Okamoto, A.; Azuma, M.; Matsuda, Y. Prevention of Red Scale Formation during Hot Rolling of Steels. ISIJ Int. **1995**, 35 (7), 886–891. https://doi.org/10.2355/isijinternational.35.886.
8. Suarez, L.; Schneider, J.; Houbaert, Y. High-Temperature Oxidation of Fe- Si Alloys in the Temperature Range 900-1250°C. Defect Diffus. Forum 2008, 273–276, 661–666. https://doi.org/10.4028/www.scientific.net/ddf.273-276.661.
9. Fukagawa, T.; Okada, H.; Maehara, Y. Mechanism of Red Scale Defect Formation in Si-Added Hot-Rolled Steel Sheets. ISIJ Int. **1994**, 34 (11), 906–911. https://doi.org/10.2355/isijinternational.34.906.
10. Liu, X.; Cao, G.; He, Y.; Jia, T.; Liu, Z. Effect of Temperature on Scale Morphology of Fe-1.5Si Alloy. J. Iron Steel Res. Int. **2013**, 20 (11), 73–78. https://doi.org/10.1016/S1006-706X(13)60199-5.
11. Young, D. High-Temperature Oxidation and Corrosion of Metal, 1st ed.; Elsevier Ltd: Oxford, **2008**; Vol. 1.
12. Logani, R.; Smeltzer, W. W. Kinetics of Wustite-Fayalite Scale Formation on Iron-Silicon Alloys. Oxid. Met. **1969**, 1 (1), 3–21. https://doi.org/10.1007/BF00609922.
13. Corish, N.; Durham, R.; Lacaze, J.; Muntean, A.; Pieraggi, B. Microstructural Observations of the Oxide Scale Growth during Short-Term Heat Treatment of Cast Irons. Int. J. Cast Met. Res. **2003**, 16 (1–3), 143–148. https://doi.org/10.1080/13640461.2003.11819573.
14. Przybilla, W.; Schütze, M. Role of Growth Stresses on the Structure of Oxide Scales on Nickel at 800 and 900°C. Oxid. Met. **2002**, 58 (1–2), 103–145. https://doi.org/10.1023/A:1016016608591.
15. Zhang, M.; Han, Y.; Zu, G.; Sun, J.; Zhu, W.; Chen, H.; Ran, X. High-Temperature Oxidation Behavior of a Cu-Bearing 17Cr Ferritic Stainless Steel. Scanning **2020**, 2020, 1–11. https://doi.org/10.1155/2020/8847831.
16. Sampson, E.; Sridhar, S. Effect of Silicon on Hot Shortness in Fe-Cu-Ni-Sn-Si Alloys During Isothermal Oxidation in Air. Metall. Mater. Trans. B **2013**, 44 (5), 1124–1136. https://doi.org/10.1007/s11663-013-9876-y.
17. Batz, W.; Mead, H. W.; Birchenall, C. E. 1952-Batz_Diffusion of Silicon in Iron. **1952**, No. August 1947, 1947.
18. Xu, Z.; Song, L.; Zhao, Y.; Liu, S. The Formation Mechanism and Effect of Amorphous $SiO_2$ on the Corrosion Behaviour of Fe-Cr-Si ODS Alloy in LBE at 550 °C. Corros. Sci. **2021**, 190 (March), 109634. https://doi.org/10.1016/j.corsci.2021.109634.
19. Mackwell, S. J. Oxidation Kinetics of Fayalite ($Fe_2SiO_4$). Phys. Chem. Miner. **1992**, 19 (4), 220–228. https://doi.org/10.1007/BF00202311.